Perivascular pathways of CSF flow through the spinal cord

Dr Alisha Sial

(MBBS)

MACQUARIE University

SYDNEY·AUSTRALIA

A thesis submitted for the partial fulfillment of the requirements for the degree of Master of Research in Faculty of Medicine and Health Sciences.

October 2015

Supervisor: Prof Marcus Stoodley[1]

Co-supervisor: Dr Sarah Hemley[1]

[1]Department of Clinical Medicine, Faculty of Medicine and Health Sciences, Macquarie University, Sydney, NSW, Australia.

Main text word count: 7935

Abstract character count: 303

Number of figures: 14

Key words: Syringomyelia; Cerebrospinal fluid; perivascular spaces; fluid outflow pathways; spinal cord; CSF tracer; in-vivo imager; immunohistochemistry.

DECLARATION OF ORIGINALITY:

I certify that the work in this thesis entitled "Perivascular pathways of CSF flow through the spinal cord", has not previously been submitted for a degree nor has it been submitted as part of requirements for a degree to any other university or institution other than Macquarie University. I also certify that the thesis is an original piece of research and it has been written by me. Any help and assistance that I have received in my research work and the preparation of the thesis itself have been appropriately acknowledged. In addition, I certify that all information sources and literature used are indicated in the thesis. The research presented in this thesis was approved by Macquarie University Ethics Review Committee, reference number: ARA 2013/047.

Dr Alisha Sial

MQ student number: 43873928

04/12/15

CONFLICT OF INTEREST STATEMENT:

The research was conducted in the absence of any commercial or financial relationships that could be construed as a potential conflict of interest.

ACKNOWLEDGEMENTS:

I would like to express my deepest gratitude to a number of people who have supported me during my MRes 2nd year. First, I would like to thank my supervisor, Professor Marcus Stoodley, for giving me this opportunity to work in this team. It has been a privilege and I am really looking forward to keep working with this group. It is your valuable advice and support that kept me inspired throughout the whole year.

I would like to thank my co-supervisor Dr Sarah Hemley for her continuous guidance, patience and encouragement throughout the year. I cannot thank you enough for sticking by me and helping me throughout difficult times. Your immerse knowledge and patience in teaching has made the learning experience worthwhile and memorable. I could not have imagined having a better co-supervisor and mentor for my Mres study.

My sincerest thanks goes Dr Magdalena Lam for always being there for me and supporting me throughout my experiments and thesis writing. My thesis would not be possible without the invaluable time you spent in improving it.

Needless to say I would like to thank the neurosurgery team for their support and advice. I would not have done this without you. A special thanks to my friends and colleagues for proof reading my work and giving feedback.

Furthermore, I would give my sincere thanks to the following staff at the Central animal Facility, Wayne, Robyn and Christine who provide help in animal care and the staff in the Department of Biomedical Sciences, Ms Lucy Lu, Ms Tamara Leo, Ms Louise Marr for their various support to ensure the research work undertaken as planned.

I acknowledge the Faculty of Medicine and Health Sciences and Macquarie University for providing me the valuable opportunity to carry out research work in such an institute with so many talented scientists.

Last but not the least I would like to thank my parents for their constant love and support without which I would not have been able to make it this far in my career.

ABSTRACT:

Syringomyelia is a condition that is characterized by fluid containing cavities within the spinal cord. It is believed that the formation of syringomyelia is linked to the imbalance in the inflow and outflow of CSF in the spinal cord. Previous studies indicate that the perivascular spaces play an important role in the fluid outflow pathways in the spinal cord. In a study of the fluid flow pathways in the brain, it was demonstrated that the fluid inflow pathways are via periarteriolar spaces and outflow is from perivenular spaces. We know these pathways exist in the brain parenchyma, however, we do not know if the same fluid outflow pathways exist in the spinal cord. The aim of this study was to investigate the CSF outflow pathways and fluid flow from the gray matter in a normal spinal cord. To achieve this we first optimized a method which allowed movement of CSF to be followed from the spinal cord parenchyma. A fluorescent tracer (Ovalbumin Alexa Fluor 647) was injected into the gray matter of the spinal cord in Sprague-Dawley rats. Immunohistochemistry was performed using Rat endothelial cell antibody and smooth muscle actin to differentiate between all the blood vessels. This study showed that this technique can be used reliably to assess the outflow pathways in the spinal cord. Contrary to previous reports of the outflow pathways in the brain, the preliminary in the spinal cord suggested that the tracer was found to label all the blood vessels in the gray matter of the spinal cord. This indicated that the outflow in the spinal cord occurred along perivenular and periarteriolar spaces and the capillaries, into the vasculature. Further work with a larger cohort is required to gain a better understanding of the outflow pathways in the spinal cord.

Keywords: Syringomyelia; Cerebrospinal fluid; perivascular spaces; fluid outflow pathways; spinal cord; CSF tracer; in-vivo imager; immunohistochemistry.

1 CONTENTS

Perivascular pathways of CSF flow through the spinal cord

INTRODUCTION

Cerebrospinal fluid (CSF) fills the large spaces within and around the central nervous system (CNS). The CSF is a clear, colorless fluid made by the choroid plexus, which is located in the cerebral ventricles at a rate of 500 mL/day (Bradley, 2015). The mammalian body comprises of two fluid compartments, namely, an intracellular compartment which contains approximately 60 – 65% of the body's water, and the extracellular (ECF) compartment which makes up the other 35 – 40% The extracellular compartment contains interstitial fluid (ISF) which in the CNS surrounds the cells in the brain and spinal cord, intravascular fluid (blood plasma) and transcellular fluid, which contains CSF. An increased production of ECF and increased resistance of bulk flow of ECF towards the subarachnoid space results in the accumulation of ECF (Greitz, 2006). Classical CSF studies demonstrated that the CSF serves as a sink to interstitial solutes, as tracers that are injected into different regions of the brain and spinal cord, drain into different CSF compartments by diffusion and bulk flow (Simon and Iliff, 2015). Diffusion describes the passage of fluid according to chemical concentration gradients. On the other hand, bulk flow consists of fluid movements according to pressure gradients (Klekamp, 2002). CSF bulk flow in a rat's brain was measured to be 0.1–0.3 μl min−1 g−1 (Abbott, 2004). It was recently discovered in a novel study that inspiration is a major regulator of human CSF flow, and only a minor component of CSF flow was ascribed to cardiac pulsations (Dreha-Kulaczewski *et al.*, 2015).

When considering the fluid balance, the CNS, can be thought of as a greatly distorted tube sealed at one end. Hence starting from the blind end, the space inside the tube includes a pair of chambers (lateral ventricles) one in each cerebral hemisphere, which is connected via the cerebral aqueduct (aqueduct of Sylvius) to the midline fourth ventricle which leads to both the central canal in the spinal cord as well as the subarachnoid spaces outside the tube. Perivascular spaces surround perforating arterioles and venules as they course from the subarachnoid space through the brain and spinal cord parenchyma. CSF is normally removed by several routes including the arachnoid villi leading to venous sinuses, perineural pathways across the cribriform plate leading to the nasal mucosa, and pathways at the roots of spinal nerves leading to either blood or lymphatics (Hladky and Barrand, 2014). The movement of CSF from para-arterial space into the interstitial space of the brain occurs through or around the endfeet of astrocytes that almost surround the microvasculature of the brain. At this anatomic site, the diffusion of CSF into the interstitial fluid

is determined in by the molecular weight of molecules in the CSF. The unidirectional flow of CSF from paraarterial space into the brain parenchyma is facilitated by water transport within the astrocytes via passive channels known as aquaporin 4.

Recently, the role of a water channel protein on CSF movement in the brain has been studied. Aquaporins are a family of integral membrane proteins which form water selective pores and are ubiquitously expressed in tissues (Vitellaro-Zuccarello *et al.*, 2005). Aquaporin 4 functions as a water-selective passive channel in glial cells throughout the CNS (Yang *et al.*, 2008). Iliff *et al* studied the role of aquaporin 4 in knockout mice in which they discovered the flow of CSF in the brain was through paravenular pathways (Iliff *et al.*, 2012). The role of AQP4 has also been studied in a spinal cord condition associated with disturbances in normal CSF flow, syringomelia (Simon and Iliff, 2015).

Syringomyelia is a progressive syndrome ranging from minimal to significant loss of neurological functions (Sharma *et al.*, 2006). These neurological deficits are particularly devastating, as the syrinx progresses, symptoms such as pain, weakness and loss of sensation develop Syringomyelia is associated with a number of abnormalities including Chiari 1 malformation, spinal trauma, spinal cord tumors and arachnoiditis (Heiss *et al.*, 1999), having a prevalence of 9 cases per 100,000 population (Chaudhary and Fehlings, 2015) , with 2,100 Americans affected annually (Sharma *et al.*, 2006). Surgical treatment of syrinxes typically involves shunt placement or removal of scar tissue around the spinal cord, but these treatments haven't been very effective with patients with post-traumatic syringomyelia (Sakushima *et al.*, 2013)

To develop better treatments for syringomyelia we first have to gain insight into the specific routes for fluid flow into and out of the normal spinal cord. Currently available methods to study the flow of fluid in the central nervous system use various tracers, such as horseradish peroxidase (Stoodley *et al.*, 1996) (Rennels *et al.*, 1990) (Brodbelt *et al.*, 2003), fluorescent molecules (Iliff *et al.*, 2012) and radiolabelled tracers (Boulton *et al.*, 1996). Horseradish peroxidase is a useful tracer used to study the inflow and outflow of fluid flow, however it does not allow macroscopic analysis, and is not ideal for double labelling immunohistochemistry studies used to identify different blood vessels. The use of radiolabelled tracers tend to make it difficult to calculate the recovery of the tracer, as they tend to give higher recoveries than usual since a significant level of radioactivity is still present in the brain when injected in the brain parenchyma (Boulton *et al.*, 1996) Iliff et al., injected small fluorescent tracers into the CSF at different sites and initially observed that tracer injected into the

lateral ventricles, which is the site of CSF production, minimally diffused into the parenchyma of the brain. While in contrast, tracer injected into the cisternal space surrounding the external surface of the brain entered the brain parenchyma. It was demonstrated that the CSF enters the brain parenchyma along perivascular spaces that surround penetrating arteries and that brain ISF is cleared along paravenous drainage pathways (Iliff *et al.*, 2012). Understanding these pathways is critical to understand disorders related to disturbances in CSF homeostasis including brain edema, hydrocephalus and syringomyelia.

In an inflow study regarding posttraumatic syringomyelia, it was observed that CSF tracers injected into the subarachnoid space move along the perivascular spaces into the spinal cord and central canal (Hemley *et al.*, 2013). However, little is known about the corresponding outflow pathways, in particular, whether or not the same paravenous outflow pathways that exist in the brain, serve a similar function in the spinal cord.

The hypothesis of this current study was that the perivenular spaces are a major outflow route for CSF from the spinal cord parenchyma to the subarachnoid space.

The aim of the study was to:

1. Develop a technique for studying CSF outflow pathways from the spinal cord gray matter.
2. Determine the CSF outflow pathways from the gray matter in the normal spinal cord.

MATERIALS AND METHODS

Ethical approval from the Animal Ethics Committee of Macquarie University was granted prior to the following study (ARA 2013/047). Experiments were initially carried out on 7 dead Sprague-Dawley rats to ascertain the exact stereotaxic coordinates for the injection of the fluorescent tracer (Ovalbumin, Alex Fluor 647 conjugate, 2mg, Life Technology: 034784) into the gray matter. Ovalbumin Alexa Fluor (AFO) along with fluorescent beads (Fluoro-Max, Thermo Scientific) was injected into the gray matter of the spinal cord. The initial experiments were carried out to ensure the tracer could be reliably injected into the gray matter of the spinal cord. Different volumes of CSF tracer were used for the injections. For the initial experiments, a volume of 2 µl was injected. This volume seemed to cause significant damage to the spinal cord parenchyma, forming a cavity, and was subsequently decreased to 1 µl.

Five male Sprague-Dawley rats that weighed 492g - 557g were used for the following study. The first successful injection animal was injected with 1 µl of AFO. This resulted in a small cavity at the injection site. The subsequent successful animal was injected with 0.5 µl of AFO. The animals were anesthetized with 5 % isoflurane (I.S.O, Veterinary companies of Australia Pty LTD, NSW, Australia) in 0.2 L/min oxygen in an induction chamber before the surgery. The rat was then placed prone, in a nose cone on a stereotaxic frame (lab standard stereotaxic, Stoelting, Dublin, Ireland) while the head was kept at the same level of the body. To maintain physiological body temperature, animals were placed on a heating pad. Isoflurane was reduced to 2 – 2.5 % according to the respiratory rate of the animal. The skin was shaved and cleaned with povidone iodine and the hind limb reflex was checked. Intraperitoneal injection of 5.0 ml/kg normal saline was injected into the rat before the incision. The incision was made from the base of the skull to the level of T2 vertebra. The subcutaneous tissue and muscles were dissected and hemostasis was secured. When the laminae were visualized, laminectomies were performed at the level of C7 and T1 vertebrae, and the spinal cord was exposed.

INTRAPARENCHYMAL INJECTION OF CSF TRACER:

A glass needle held in a stereotactic micromanipulator was used for the injection of the CSF tracer into the spinal cord. A 30 gauge needle was used to puncture the dura prior to the injection into the dorsal cord parenchyma along the right dorsal nerve rootlets between the rostral C8 and caudal T1 spinal level. The injection site for the first rat was 0.5 mm to the right of the dorsal spinal vein, which was used as the midline. Using a glass micropipette, 1 µl of fluorescent tracer was injected into the spinal cord at a depth of 1 mm over 2 minutes 39 seconds. The glass micropipette was left in place for an additional 5 minutes, after which it was retracted 0.5 mm and left in the cord for 60 minutes before perfusion. The injection site for the second rat was identical to the first, 0.5 mm right of the dorsal spinal vein, with a depth of 1 mm. The tracer was injected over 4 min 20 sec. The needle was retracted 0.5 mm and then left in situ for the next 60 minutes.

Tracer leakage was observed in the subarachnoid space during the injection in both the rats. Once the needle was retracted 0.5 mm, at approximately 20 minutes post-injection, it appeared that the spinal pulsations had pushed the fluid (a mix of fluorescent tracer and CSF) back into the glass micropipette. At 60 minutes, intracardiac perfusion of the rat was performed with 0.1 M phosphate buffer solution (PBS) containing 5000 IU of heparin (Hospira Australia Pty, LTD, Melbourne, VIC, Australia) and 4 % paraformaldehyde (PFA), for 20 minutes at the rate of 50 ml/min.

MULTISPECTRAL IMAGING SYSTEM:

After successful perfusion, the spinal cord was removed and viewed in the In-Vivo MS FX PRO imaging system. Multispectral dorsal and ventral imaging of the whole brain and spinal cord was done under white light in order to identify the spinal segments. The intensity of the CSF tracer was detected at an excitation wavelength of 620 nm and emission wavelength of 700 nm. Fluorescent images of whole spinal cord were captured with an exposure time of 4 seconds on both, dorsal and ventral, sides. After the images were taken the spinal cord was divided into segments. Tissue was subsequently cut into segments as follows: C2, C4, C6, C7 to T1, T2, and T4 (C refers to cervical and T refers to thoracic spinal cord) and kept overnight in 4 % PFA. The next day. The spinal segments were then placed in molds in OCT compound (ProSciTech Pty Ltd, QLD, Australia), they were then snap frozen using liquid nitrogen and stored at -80˚C. Then 40 µm sections were cut using a cryostat (Leica, Wetzlar, Germany).

IMMUNOHISTOCHEMISTRY:

The cryostat sections were placed on glass slides and then placed in the oven for 20 minutes at 37˚C. The slides were then washed twice for 10 minutes each in tri-phosphate buffered saline (TPBS) pH 7.4 to remove OCT, and then placed in a solution of 50 % ethanol in TPBS on a stirrer for 20 more minutes. The slides were then washed three times for 10 minutes each in TPBS to remove the ethanol. The slides were placed in long humidifiers and the blocking solution using 15% normal donkey serum (NDS) in TPBS, was added. Slides with the blocking solution were incubated in the humidifiers for 60 minutes. After 60 minutes, the blocking solution was tapped off from the slides, Rat Endothelial Cell Antibody (1:100; RECA-1 AB9774 Abcam, Cambridge, United Kingdom) and anti-actin α-smooth muscle antibody conjugated to Cy3 (1:400 dilution SMA-Cy3 C6198, Sigma-Aldrich, St. Louis, Montana), were added on the slides and left for incubation overnight at 4˚C.

The next day, the slides were kept at room temperature for 2 hours and then the primary antibodies were washed off in TPBS. Secondary antibody, 1:400 diluted secondary anti-mouse IgG Alexa Fluor 488 (Molecular Probes, Life Technologies, New York, USA) in 4 % NDS/TPBS solution was added to the slides and left at room temperature for 2 more hours. After 2 hours incubation, the secondary antibody was then tapped off and the slides were cover-slipped with fluorescent

mounting medium (DAKO, S3023, NSW, Australia) and imaged on a Zeiss Z1 (Gottingen, Germany) microscope.

IMAGE ANALYSIS:

Macroscopic image analysis:

Fluorescent images were taken of the whole brain and spinal cord, which were later converted to black and white images. The measurements of the fluorescent tracer in the spinal cord were taken at each spinal level. In order to localize the distribution of the CSF tracer in the spinal cord parenchyma, photomicrographs were split into different fluorescent channels. The Cy5 channel was used to visualize the CSF tracer. In order to acknowledge the CSF tracer intensity, Image-J software was used. The background fluorescence was subtracted using a region of interest outside the spinal cord. The image was thresholded and the integrated density was determined. The integrated density is a measure of the number of fluorescent pixels per unit area.

Microscopic image analysis:

To determine the distribution of CSF tracer in relation to the microvasculature in the spinal cord, the blood vessels surrounded by the CSF tracer were counted using the Carl-Zeiss Zen microscope software. The fluorescent beads were used to verify the location of the injection site. SMA-positive vessels were identified as arterioles. SMA-negative, RECA-positive vessels were considered to be venules and capillaries. In order to distinguish between venules and capillaries, their largest diameters were measured. Vessels $\geq$ 6.5 µm were identified as venules, those $\leq$ 6.5 µm were identified as capillaries.

RESULTS

Five male Sprague-Dawley rats were used for the in-vivo study. The first rat died during surgery and was excluded from the study. In the second rat, the injection of 1 µl of CSF tracer caused significant damage to the spinal cord and this animal was also excluded from the study. The third rat was also injected with 1 µl of CSF tracer, however, the tracer was not visualized in the right gray matter and was only observed in the periphery hence making this experiment void. The two subsequent rats were injected successfully and are discussed here.

Rat with 1 µl CSF tracer injected:

The brain and spinal cord along with the spinal roots were visualized under the white light in order to determine the localization of the CSF tracer along the different spinal levels (**Figure 1**). The highest intensity was observed predominantly on the dorsal side of the spinal cord at the level of C7-T1, which corresponds to the injection site (**Figure 2**). Some CSF tracer intensity was seen in the level of C6 on the dorsal side. There was some tracer detected at the level of C7-T1 in the ventral side of the spinal cord, but it was not as much as on the dorsal side. The tracer intensity measured is consistent with the injection site.

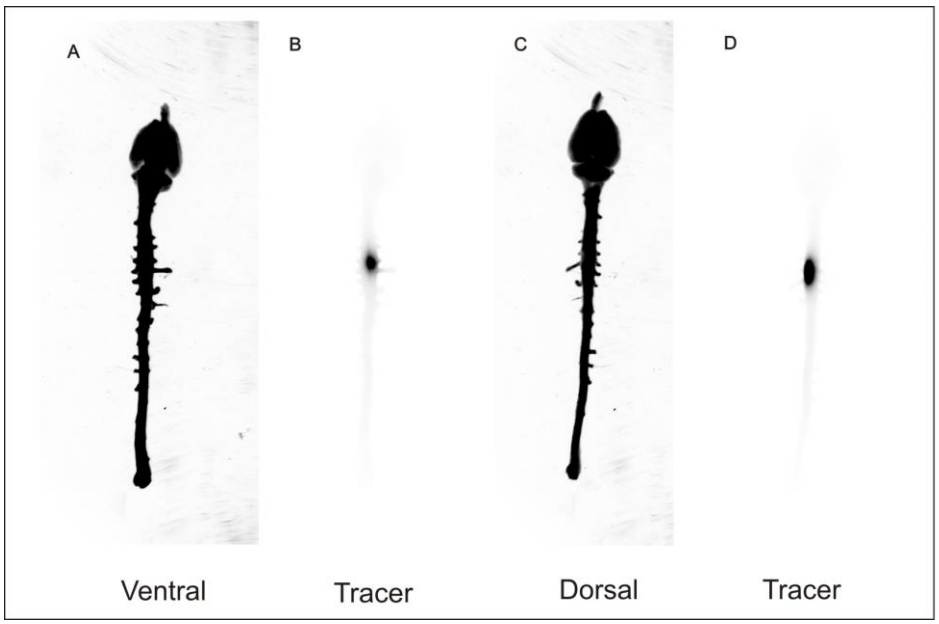

Figure 1 *Rat with 1 µl of CSF tracer injected. Visualization of CSF tracer in the spinal cord using In-Vivo MS FX PRO. (A and C) Ventral and Dorsal side of the spinal cord under white light. (B and D) CSF tracer distribution in the ventral and dorsal side of the spinal cord respectively.*

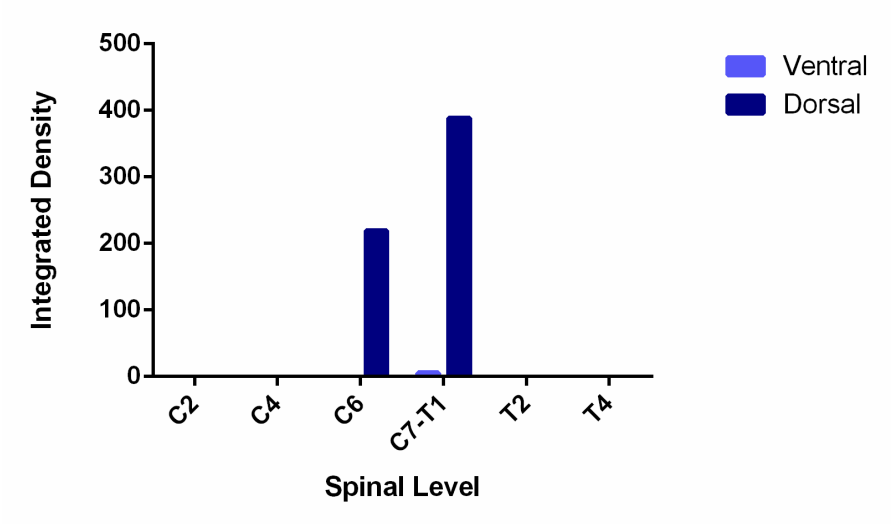

Figure 2 *CSF tracer intensity measured from ventral and dorsal images of the spinal cord.*

Rat with 0.5 µl CSF tracer injected:

The brain and spinal cord of the second rat with 0.5 µl of CSF tracer injected was visualized under the white light and fluorescent images were taken (**Figure 3**). The highest tracer density was measured at the ventral side of the spinal cord at the level of C7-T1. However, there was a significant amount of tracer intensity measured at the dorsal side of the spinal cord (**Figure 4**).

The CSF tracer intensity in the first rat, with a higher volume of CSF tracer injected, was higher on the dorsal side, however, this was not the case in the second rat with the lower volume of CSF tracer injected. The second rat showed more fluorescence in the ventral side of the spinal cord. There was no evidence of the tracer above and below the level of the injection site.

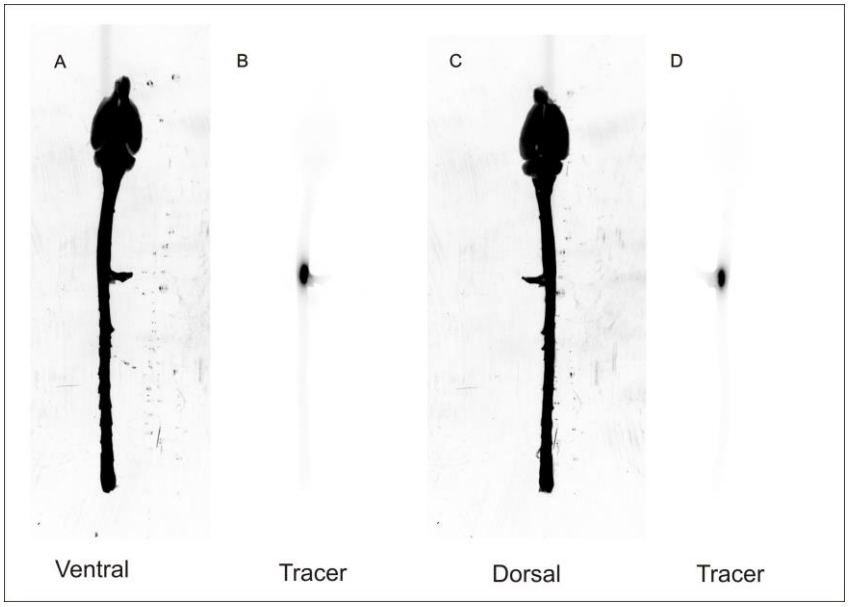

Figure 3 *Rat with 0.5 µl of CSF tracer injected. Visualization of CSF tracer in the In-Vivo MS FX PRO. (A and C) Ventral and Dorsal sides of the spinal cord in the white light. (B and D) show the CSF tracer in the spinal cord.*

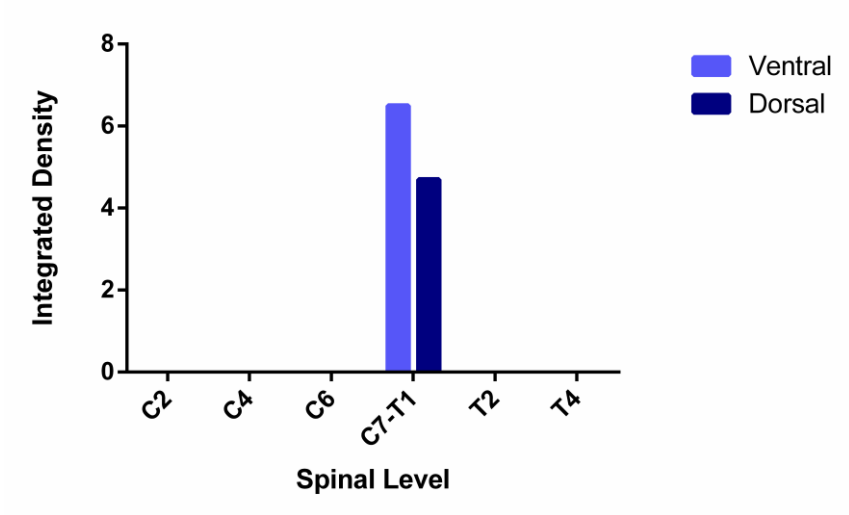

Figure 4 *CSF tracer intensity measured at the spinal levels at ventral and dorsal sides of the spinal cord.*

Microscopic analysis:

The injection site of both the rats was in the right gray matter of the spinal cord. Successful injection of the CSF tracer was verified by injecting fluorescent beads mixed with the CSF tracer. A cavity was observed at the injection site of the first rat with 1 µl of CSF tracer injected (**Figure 5)**. These

beads were spread over 11 sections of the injection site segment. However, in the second rat, 0.5 µl of CSF tracer injected, there was no cavity observed. The beads were present in 9 sections of the injection site segment (**Figure 6**).

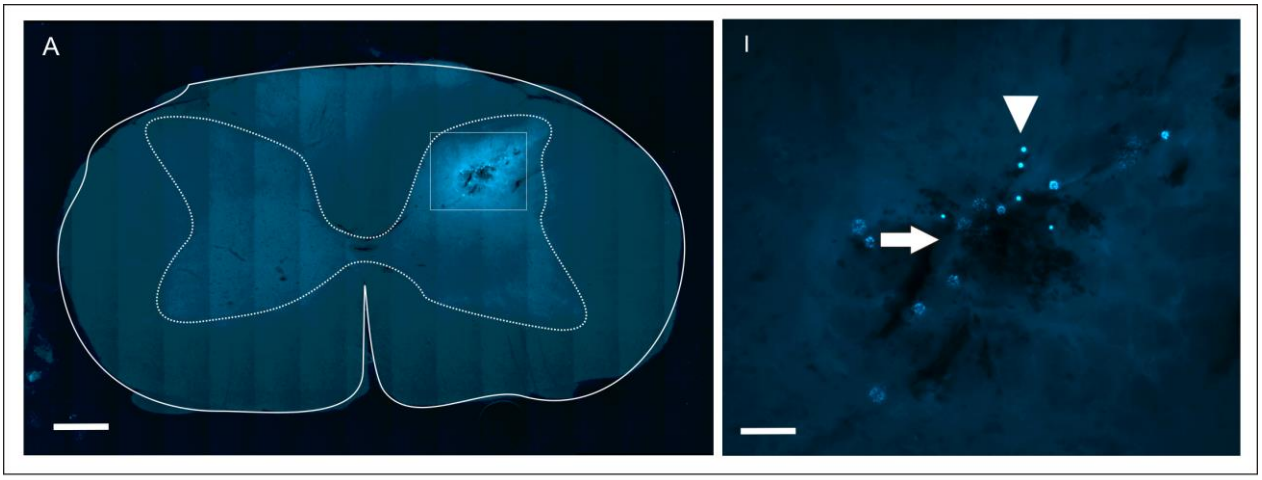

Figure 5 *Cross-section of the spinal cord of the rat with 1 µl of CSF tracer injected in the right gray matter of the spinal cord (A).[Dotted lines denote the gray matter.] An enlarged view of the inset is seen in (i?) showing a cavity in the parenchyma of the right gray matter (Arrow). Localization of the injection site was determined by fluorescent beads (Arrowhead). (Scale bar A = 200 µm; Scale bar i = 50 µm)*

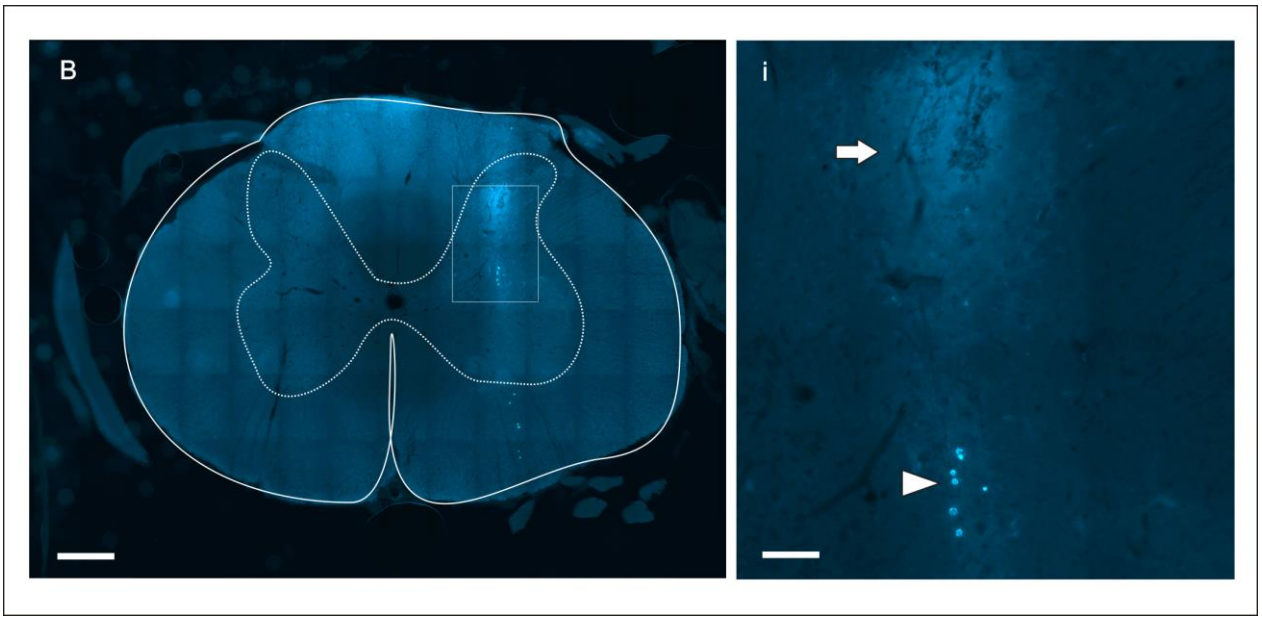

Figure 6 *Cross-section of the spinal cord of the rat with 0.5 µl of CSF tracer injected in the right gray matter (B). [Dotted lines denote the gray matter] An enlarged view of the inset (i) indicates*

the injection site (Arrow). Fluorescent beads (Arrowhead) were used to localize the injection site. (Scale bar B = 200µm; Scale bar i = 50 µm)

Rat with 1 µl of CSF tracer injected:

The CSF tracer was successfully injected in the right gray matter of the spinal cord. Tracer was observed surrounding arterioles, venules and capillaries (**Figure 7**).

Rat with 0.5 µl of CSF tracer injected:

The tracer was observed in the right gray matter of the spinal cord of the second rat. Similar to the first rat, the tracer was observed surrounding arterioles and surrounding the venules (**Figure 8**).

Collectively, these results show that at 60 minutes post injection, the CSF tracer was observed in the central gray matter. The fluorescent tracer distributed predominantly in a diffuse manner throughout the right and central gray matter, however it was also observed labelling all the blood vessels with comparable staining of arterioles, venules and capillaries. When 1 µl of CSF tracer was injected in the right gray matter of the spinal cord, a cavity was observed. This was not the case in the second rat in which 0.5 µl of tracer was injected.

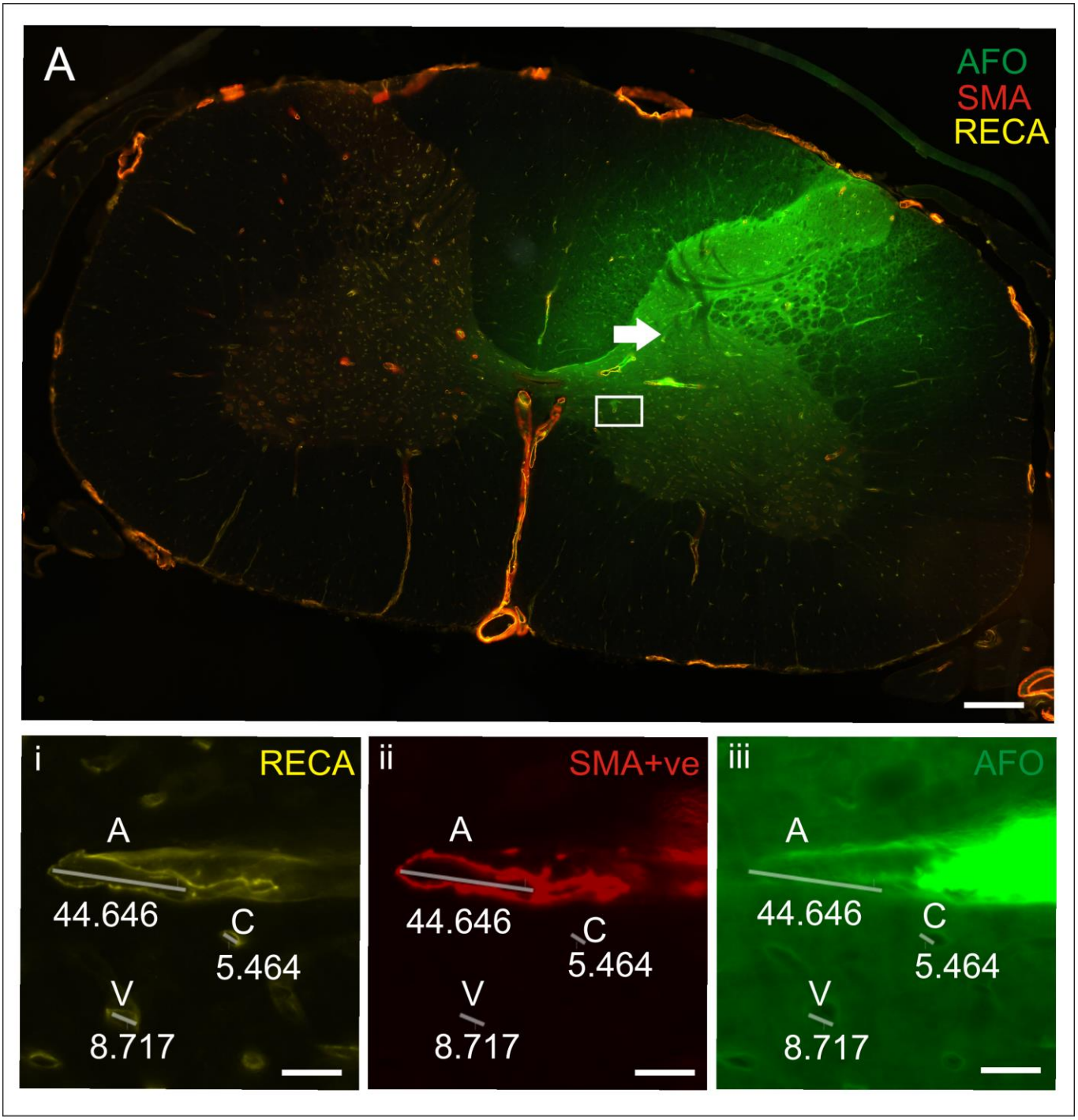

Figure 7 Rat with 1 µl of CSF tracer injected in the right gray matter. (A) Shows the injection site in the right gray matter (Arrow). (i, ii and iii) Enlarged view of the subset in A. (i) shows RECA staining of all the blood vessels. (ii) Shows SMA staining of the arterioles. (iii) Shows the CSF tracer present around the blood vessels labelled as A, V and C. (A – Arterioles, V – Venules, C – Capillaries) (Scale bar A = 200 µm ; Scale bar i,ii,iii = 50 µm)

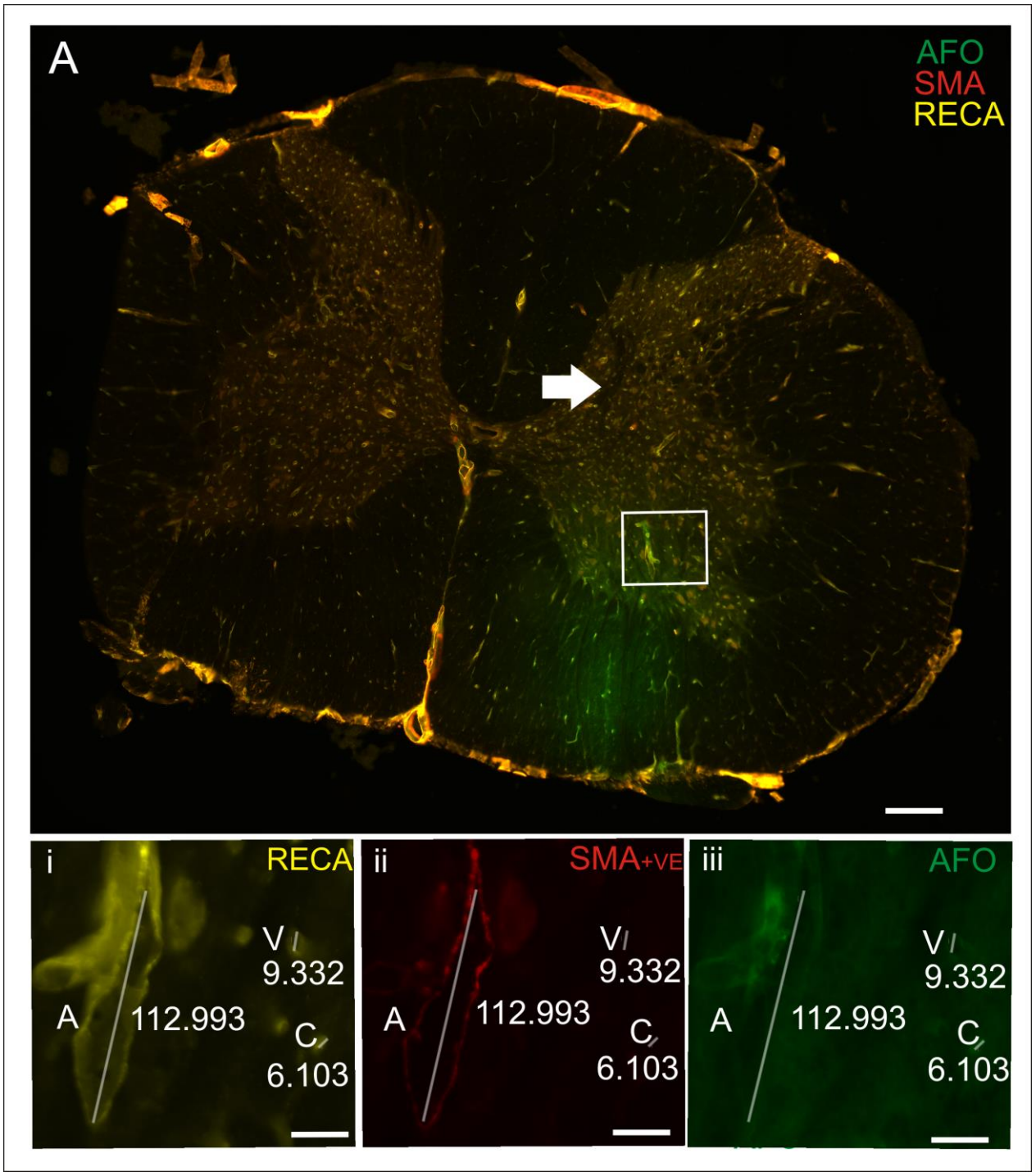

Figure 8 Rat with 0.5 of CSF tracer injected in the right gray matter. Representative images of the spinal cord at C8. (A) Shows the injection site in the right gray matter (Arrow). (i, ii and iii) Enlarged view of the inset in A. (i) shows RECA staining of all the blood vessels. (ii) Shows SMA

staining of arterioles. (iii) Shows the CSF tracer around all the blood vessels. (Scale bar = 200 µm; Scale bar i,ii,iii = 50µm)

Rat with 1 µl CSF tracer injected:

CSF tracer was observed in the periphery and around the central canal of the C5 spinal segment, with only arterioles labeled with the CSF tracer (**Figure 9**). The injection site was at C7-T1 (e-f). Rostral to the injection site, C7-T1 (a-c), there was localization of tracer around the arterioles predominately in the right gray matter around the right dorsal horn. Moving closer to the injection site, C7-T1 (d), the tracer was observed around the arterioles in the left gray matter, right and left dorsal white matter and some in the right white matter. The venules labeled with CSF tracer, were predominantly observed around the central canal and right gray matter. However some tracer was observed in the left gray matter as well. The capillaries labeled with CSF tracer were around the central canal and right gray matter and the right dorsal white matter.

At the injection site, C7-T1 (e-f), staining of arterioles labeled with CSF tracer was predominantly similar in the right and left gray matter although some labeled arterioles were also observed in the right white matter closer to the right dorsal horn. Venules labeled with CSF tracer were observed mostly around the central canal and the right gray matter. However moving caudally from the injection site the venules labeled with tracer were dispersed around the right and left gray matter. Capillaries labeled with CSF tracer were observed only in the right and left gray matter, only a few of them were seen in the ventral horn of the right white matter.

Caudal to the injection site, C7-T1 (h-j), a similar number of arterioles surrounded by CSF tracer were observed in the right and left gray matter. Some arterioles labeled with CSF tracer were seen in the right white matter as well. Venules labeled with CSF tracer were observed in the right and left gray matter and to a lesser extent in the right white matter. However very few venules with CSF tracer were observed in the left white matter. Capillaries labeled with CSF tracer were observed in the right and left gray matter, some tracer labelled capillaries were observed in the right white matter and the right and left dorsal white matter. As the CSF tracer, decreased caudally, the capillaries and venules labeled with tracer were observed in the right and left dorsal white matter, right white matter and in the right gray matter.

At T2-T4 there was no tracer observed in arterioles, venules or capillaries.

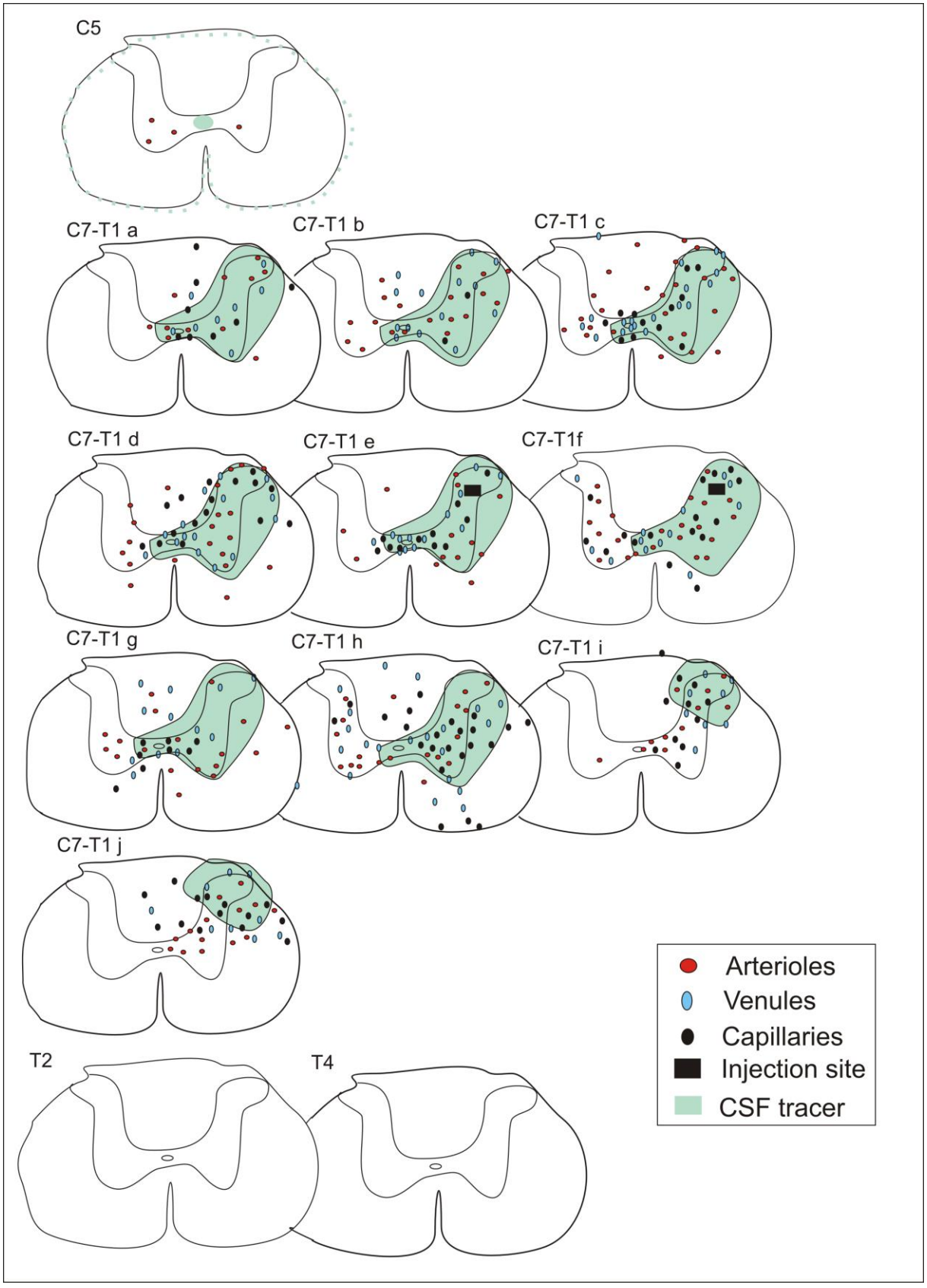
C5
C7-T1 a
C7-T1 b
C7-T1 c
C7-T1 d
C7-T1 e
C7-T1f
C7-T1 g
C7-T1 h
C7-T1 i
C7-T1 j
T2
T4
Arterioles
Venules
Capillaries
Injection site
CSF tracer

Figure 9 Schematic diagram of the rat with 1 µl of CSF tracer representing the localisation of CSF tracer around the blood vessels.

Rat with 0.5 µl CSF tracer injected:

There was no CSF tracer observed in different segments far rostral to the injection site, C5 segment (**Figure 10**). However in the segment C7-T1, in sections rostral to the injection site the CSF tracer was observed in the right dorsal horn of the gray matter in C7-T1 (a-b).

Arterioles labeled with CSF tracer were predominately observed in the right gray matter. Moving closer towards the injection site, C7-T1 (e), arterioles labeled with tracer were seen in the right gray matter closer to the central canal. Some arterioles labeled with tracer were localized in the right white matter as seen in C7-T1 (c), (d) and (e).

The labeling of venules with CSF tracer was predominantly the same in the right gray matter closer to the central canal and the dorsal and ventral horn of the right gray matter. Some venules labeled with CSF tracer were also localized in the right white matter and in the right dorsal white matter, C7-T1 (c), (d) & (e). Capillaries labeled with CSF tracer were predominantly in the right white matter and the right gray matter.

At the level of the injection site, C7-T1 (f) and (g), arterioles labeled with the CSF tracer were observed around the central canal and the right gray matter closer to the injection site. Some arterioles were also observed in the right dorsal horn of the gray matter. Venules labeled with CFS tracer, were predominantly localized around the central canal and the right gray matter, some venules were observed in the right white mater. Capillaries labeled with CSF were usually localized in the right gray matter and right dorsal white matter and around the central canal as seen in C7-T1 (f) & (g).

Caudal to the injection site, C7-T1 (h), arterioles labeled with CSF tracer were localized in the central canal, right gray matter and right white matter. As the CSF tracer decreased in the spinal segments caudal to the injection site, C7-T1 (i) & (j), arterioles were observed in the left and right gray matter. Venules labeled with CSF tracer were predominately seen in the right gray matter, right dorsal white matter and right white matter. As the tracer decreased down the spinal segments, venules labelled with tracer were observed mostly in the ventral horn of the right gray matter C7-

T1 (j). Capillaries labeled with CSF tracer were seen in the right gray matter, right dorsal white matter and around the central canal.

Consistent to the rat with a higher volume, 1 µl, there was no CSF tracer seen around the blood vessels at the levels of T2 and T4.

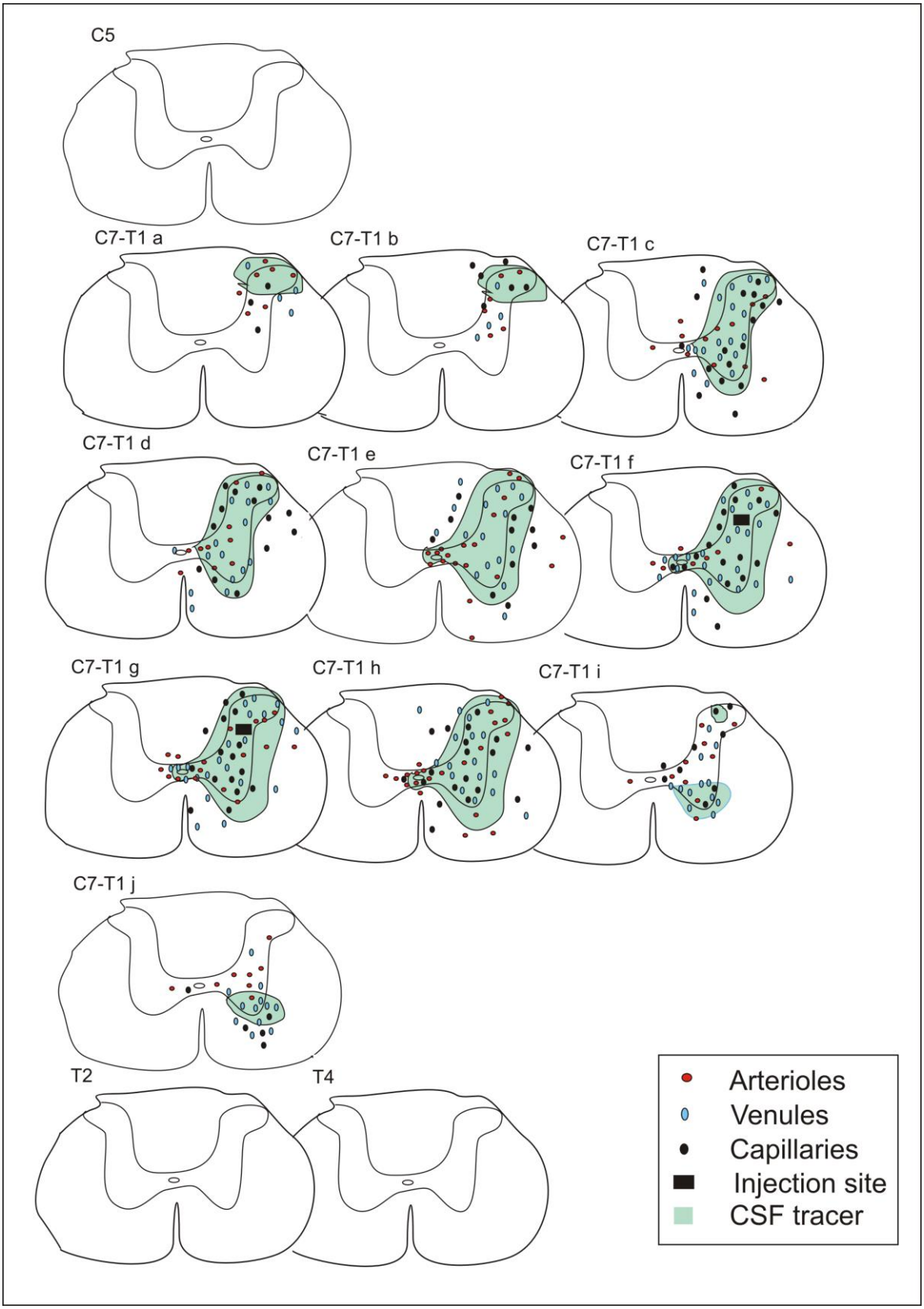
C5
C7-T1 a
C7-T1 b
C7-T1 c
C7-T1 d
C7-T1 e
C7-T1 f
C7-T1 g
C7-T1 h
C7-T1 i
C7-T1 j
T2
T4
Arterioles
Venules
Capillaries
Injection site
CSF tracer

Figure 10 Schematic diagram of the rat with 0.5 µl of CSF tracer injected, representing the localization of tracer around all the blood vessels.

Rat with 1 µl CSF tracer injected:

Microscopic analysis of the distribution in the spinal cord of the rat injected with 1 µl of CSF tracer was carried out on the alternate segments of the spinal cord and consecutive sections at the injection site (**Figure 11**). The Graph (**Figure 11**A) shows the differences in tracer densities at the different spinal levels. At the injection site, C8, the distribution of CSF tracer is found maximum in the right gray matter, which is consistent with the injection site. In the right white matter, right dorsal white matter and the central canal a higher tracer intensity was observed. Rostral to the injection site, C7-C8, most of the CSF tracer was observed in the right gray matter, right white matter, and right dorsal white matter and in the central canal respectively. This tracer intensity was lower than that at the level of C8. Caudal to the injection site, the intensity of the CSF tracer was found to be similar to that in the rostral side, but slightly lower. The highest tracer intensity was observed in the right gray matter, followed by the right white matter and right dorsal white matter. However, negligible distribution of CSF tracer was observed in the left side of the spinal cord.

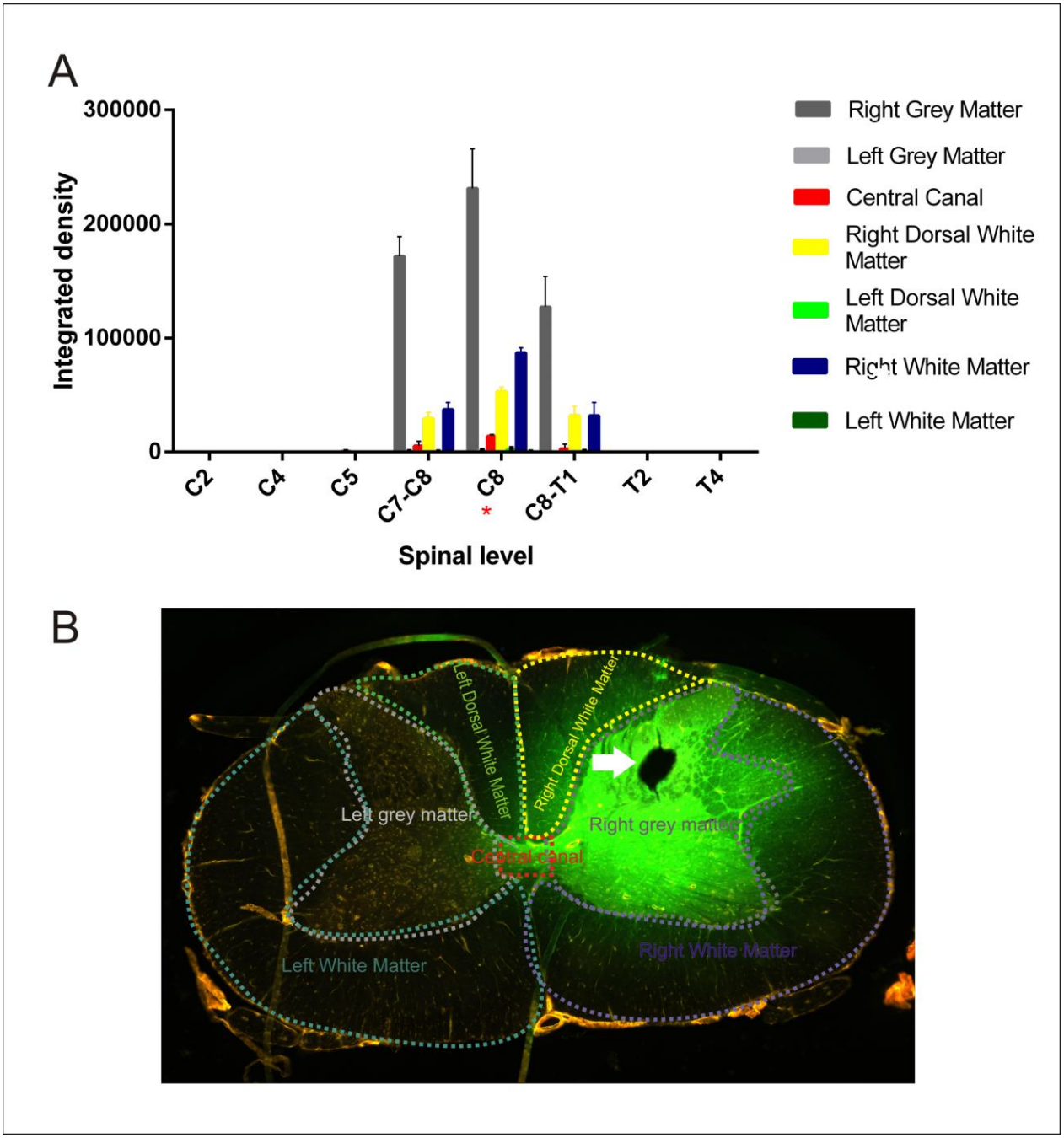

Figure 11 Analysis of CSF tracer distribution Analysis of CSF tracer distribution in different areas of the spinal cord of the rat with 1µl of CSF tracer. (A) Shows the graph of the tracer density with each spinal level. (illustrates the injection site). (B) Shows the CSF tracer intensity measured in the regions marked by dotted lines. (Arrow) shows the injection site.*

Rat with 0.5 µl of CSF tracer injected:

The analysis of CSF tracer in the spinal cord of the animal injected with 0.5 µl of AFO was carried out, illustrating the differences of the CSF tracer distribution at the different spinal levels (**Figure 12**). The maximum intensity of CSF tracer was at the injection site, C8, in the right white matter, followed by the right gray matter, right dorsal white matter and the central canal. Rostral to the injection site, C7-C8, the CSF tracer distribution was found to be higher in the right gray matter followed by right white matter. Tracer was also evident in the right dorsal white matter. Caudal to the injection site, C8-T1, the tracer intensity was measured to be comparatively less in the right white matter and right gray matter. Almost negligible levels of CSF tracer was observed in the left gray matter, left dorsal white matter, and in the left white matter (**Figure 12** A).

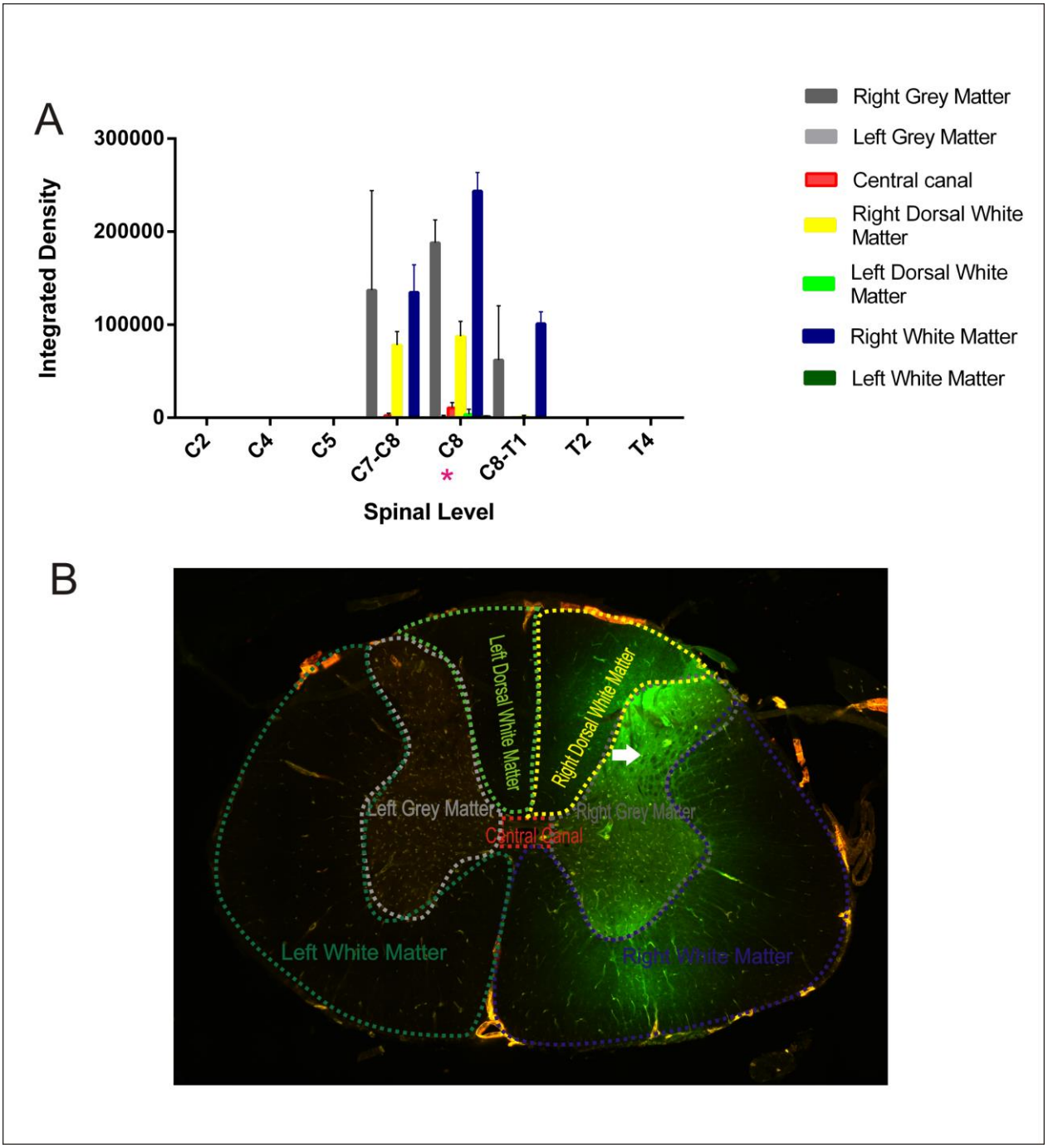

Figure 12 Analysis of CSF tracer distribution in different areas of the spinal cord of the rat with 0.5 of CSF tracer. (A) Shows the graph of the tracer density with each spinal level. (illustrates the injection site) (B) Shows the tracer intensity measured in the regions marked by dotted lines. (Arrow) shows the injection site.*

DISCUSSION

This study was primarily carried out to optimize a technique to study the fluid outflow pathways from the spinal cord gray matter. This study demonstrated that an injection site, 0.5 mm from the midline and at a depth of 1 mm enabled tracer to be reliably injected into the dorsal horn gray matter of the spinal cord. A volume of 0.5 µl of CSF tracer was found to be optimal, allowing fluid flow to be detected macroscopically and microscopically without causing significant damage to the spinal cord. Although no conclusions can be drawn from this study given the small number of animals, the preliminary results of this novel study suggest that the fluid outflow in the spinal cord gray matter occurs via peri-arteriolar and peri-venular spaces, and across the basement membrane of capillaries. This finding is contrary to the hypothesis and similar studies in the brain.

CSF FLOW IN THE CNS:

Movement of CSF tracers from the subarachnoid space into the spinal cord perivascular spaces =was first demonstrated by Brierley in 1950 (Brierley, 1950). More recently studies have shown that horseradish peroxidase injected into the subarachnoid space rapidly labels the perivascular spaces of the brain and spinal cord (Wagner *et al.,* 1983). Rennels *et al* proposed that a paravascular fluid circulation exists in the nervous system with an active flow of CSF from the subarachnoid space into the perivascular spaces around arterioles and continuing through the basal lamina around capillaries. It was proposed that this flow may have a similar role as the lymphatic function of the nervous system (Rennels *et al.*, 1985).. Fluid flow in the spinal cord has previously been investigated using horseradish peroxidase as a CSF tracer. The horseradish peroxidase reaction product was found in between perivascular spaces and the central canal, suggesting that in the spinal cord the flow may be by the perivascular spaces, the central canal and the surrounding gray matter due to the rapid diffuse labelling of these structures (Milhorat *et al.,* 1991) (Stoodley *et al.*, 1996). In another study, investigating the CSF flow in syringomyelia, it was demonstrated that the CSF flows within the spinal cord along perivascular spaces to the central canal [ref], and it has been recently postulated that variation of patency of the central canal may play an important role in the development of syringomyelia (Brugieres *et al.,* 2000). A study similar to the current study, was done by Iliff *et al* in which they identified a brain-wide pathway for fluid transport in mice. They found that the subarachnoid CSF circulates into and out of the brain interstitium along perivascular spaces, entering via surrounding cerebral arteries, and the interstitial solutes are

cleared from the brain along the perivascular channels surrounding the draining veins (Iliff *et al.*, 2015). This study was done to look at the CSF pathways in the brain, we do not know if the same pathway exists in the spinal cord.

There are anatomical differences between the brain and the spinal cord which makes us wonder whether the fluid outflow pathways are different. Contrary to previous reports of the paravascular outflow pathways in the brain which were demonstrated by Iliff *et al,* it was observed that even though the gray matter of the spinal cord has an abundance of capillaries, CSF tracer was not preferentially distributed only around capillaries. Instead it was observed in all the blood vessels in approximately equal numbers. This suggests that the outflow pathways are not limited to just arterioles, venules or capillaries. In a recent study similar to this current study was done using the same concept of spinal cord injection to determine the properties of convective delivery in the spinal cord gray matter. Evans blue dye was injected in the T-9 segment, in the gray and white matter, at the rate of 0.2 µl/min with the volume of 2 µl. It was observed that the dye was distributed exclusively in the while matter and travelled longitudinally. In contrast, in the gray matter, the dye infiltrated into the adjacent white matter and travelled along the white matter (Endo *et al.*, 2015).

The microscopic analysis of the first rat, at the level of C5, revealed that the CSF tracer was only seen in peripheral region of spinal cord and it could be due to the fact that during the injection of the tracer into spinal cord through glass micropipette, there was some reflux of the fluid around the subarachnoid space of the spinal cord. This staining at C5 was not present in the second rat (0.5 µl of tracer injected). Rostral to the injection site, arterioles, venules and capillaries labeled with CSF tracer were observed with arterioles being more predominant, which suggests that the flow of CSF rostral to the injection site occurs predominantly via periarterial spaces. However, getting closer to the injection site and caudal to the injection site, there was an increasing abundance of venules and capillaries labeled with CSF tracer. This could suggest the outflow pathway in the spinal cord occurs via perivenular spaces and via capillaries. Some venules and capillaries labeled with CSF tracer were also observed in the right white matter of the spinal cord at the injection site and a fairly low amount of CSF tracer was observed in the left side of the spinal cord, thereby suggesting the outflow pathways could be through the central canal as most of the tracer was observed around the central canal, and negligible tracer is observed on the left side of the spinal cord. This is indicative of limited lateral movement of fluid through the spinal cord parenchyma. This is supported by the fact that there was no CSF tracer observed in the caudal segments of T2 and T4,

suggesting no flow of fluid via perivascular spaces down the cord. Although there is also a possibility that the fluid could have been cleared at the glia limitans externa and into the subarachnoid space. These findings are almost consistent with the second rat with the 0.5 µl of CSF tracer injected.

LIMITATIONS OF THE STUDY:

Experiments were carried out to optimize the volume of tracer. The first rat died during surgery due to anaesthetic complications. In the second rat, the volume of tracer injected caused severe damage to the spinal cord parenchyma which could be due to either the rate of injection or the volume of the tracer. In the third rat, the CSF tracer was only localized in the periphery of the cord, no tracer was observed in the gray matter. These animals were hence excluded from the study. The two rats with successful CSF tracer injected into the gray matter of the spinal cord are discussed in this study. It was difficult to pierce the dura with a 30 gauge insulin syringe needle, prior to the insertion of the glass micropipette into the spinal cord to inject the CSF tracer. If the opening created by the insulin syringe was too large, there would be significant leakage of CSF in the subarachnoid space making it difficult to inject the right amount of CSF tracer and it could give varying results. Previous studies showed the same problem regarding microscopic evidence of transneuronal labelling using horseradish peroxidase to trace somatosensory pathways to the thalamus (Peschanski and Ralston, 1985). The location of the injection is an important factor in this study therefore making a standardized piercing in the dura, 0.5 mm to the right of the dorsal vein with a depth of 1 mm, important in localizing the site of the right gray matter of the spinal cord. The normal flow of CSF is a closed system, by piercing the dura and the subarachnoid space, it disrupts the normal physiological fluid flow of CSF. Due to this, there might be a possibility that the CSF tracer volume injected would not be very accurate. In order to optimize the technique of injecting the correct volume of CSF tracer, the appropriate volume of the tracer was to be determined. A large volume of the CSF tracer would cause significant damage to the spinal cord parenchyma, due to increased pressure, which is why two different volumes were used. Initially, in the dead rats, 2 µl of tracer was injected in the spinal cord, which caused significant damage to the spinal cord parenchyma. Thereby reducing the volume of the CSF tracer gave favorable results. The rate at which the tracer was injected was also very important, because a faster rate could cause damage to the spinal cord tissue and could lead to tracer reflux. It was rather difficult to inject the tracer slowly manually. When the glass micropipette was inserted into the spinal cord, it created

some form of resistance in the cord thereby making it difficult to inject the full volume of CSF tracer in the cord. There was movement of CSF into the glass micropipette once it was inserted into the cord, which could be due to the physiological fluid pressure and normal pulsations of the spinal cord while the rat is breathing.

The most important potential shortcoming of this work was the reflux of CSF into the glass micropipette. This was a problem as some of the CSF tracer was visualized in the subarachnoid space and on the dura. Nevertheless, the constant flow of CSF flushed some of the tracer away from the injection site once it was injected. Some of the CSF would flow into the glass micropipette making the volume of fluid in the glass micropipette larger and thereby diluting the CSF tracer.

FUTURE DIRECTIONS*:*

The role of aquaporin 4 needs to be investigated in the spinal cord in order to understand its association with the progression of syringomyelia. More work on the CSF outflow following administration of an aquaporin 4 antagonist in Sprague Dawley rats and the effect of obstruction of CSF on the CSF flow needs to be done to understand the mechanism of fluid outflow in syringomyelia.However, with regards to the fluid pathways, the results are still inconclusive as the sample size is quite low. In the future, further work will be done on a larger cohort using the CSF tracer volume of 0.5 µl which will help in determining the outflow of the fluid from the spinal cord.

The role of aquaporin 4 needs to be investigated in the spinal cord in order to understand its association with the progression of syringomyelia. Along with that, more work on the CSF outflow following administration of an aquaporin 4 antagonist in Sprague dawley rats and its effect on obstruction of CSF flow needs to be done to understand the mechanism of fluid outflow in syringomyelia. Together these studies will lead to a better understanding of normal CSF physiology and pathologies such as syringomyelia.

CONCLUSIONS:

In this current study we optimized a technique for the injection of fluorescent tracer into the spinal cord of a live rat in order to determine the pathways of CSF outflow in the spinal cord of a normal rat. The results of this study indicate that 0.5 µl of the CSF tracer injection into the gray matter of the spinal cord of the rat is most reliable for a favorable outcome for the spinal cord injection causing least amount of damage to the spinal cord parenchyma. Previous studies in the brain

showed the role of paravenular pathways in the outflow of fluid in the brain, however, this was not the case in the spinal cord. The preliminary results of this current study suggest that the outflow pathways for CSF tracer in the spinal cord are different from the outflow pathways in the brain. All the blood vessels, arterioles, venules and capillaries play an important role in the fluid outflow pathways, contradicting the hypothesis made initially.

REFERENCES

Abbott, N. J. (2004). Evidence for bulk flow of brain interstitial fluid: significance for physiology and pathology. *Neurochem Int* 45**,** 545-52. doi: 10.1016/j.neuint.2003.11.006.

Boulton, M., et al. (1996). Drainage of CSF through lymphatic pathways and arachnoid villi in sheep: measurement of 125I-albumin clearance. *Neuropathol Appl Neurobiol* 22**,** 325-33.

Bradley, W. G., Jr. (2015). CSF Flow in the Brain in the Context of Normal Pressure Hydrocephalus. *AJNR Am J Neuroradiol* 36**,** 831-8. doi: 10.3174/ajnr.A4124.

Brierley, J. B. (1950). The penetration of particulate matter from the cerebrospinal fluid into the spinal ganglia, peripheral nerves, and perivascular spaces of the central nervous system. *J Neurol Neurosurg Psychiatry* 13**,** 203-15.

Brodbelt, A. R., et al. (2003). Altered subarachnoid space compliance and fluid flow in an animal model of posttraumatic syringomyelia. *Spine (Phila Pa 1976)* 28**,** E413-9. doi: 10.1097/01.BRS.0000092346.83686.B9.

Brugieres, P., et al. (2000). CSF flow measurement in syringomyelia. *Ajnr: American Journal of Neuroradiology* 21**,** 1785-92.

Chaudhary, B. R. and Fehlings, M. G. (2015). Adult-onset syringomyelia: from theory to practice and beyond. *World Neurosurg* 83**,** 462-3. doi: 10.1016/j.wneu.2014.08.033.

Dreha-Kulaczewski, S., et al. (2015). Inspiration is the major regulator of human CSF flow. *J Neurosci* 35**,** 2485-91. doi: 10.1523/JNEUROSCI.3246-14.2015.

Endo, T., et al. (2015). Properties of convective delivery in spinal cord gray matter: laboratory investigation and computational simulations. *J Neurosurg Spine***,** 1-8. doi: 10.3171/2015.5.SPINE141148.

Greitz, D. (2006). Unraveling the riddle of syringomyelia. *Neurosurgical Review* 29**,** 251-63. doi: DOI 10.1007/s10143-006-0029-5.

Heiss, J. D., et al. (1999). Elucidating the pathophysiology of syringomyelia. *J Neurosurg* 91**,** 553-62. doi: 10.3171/jns.1999.91.4.0553.

Hemley, S. J., et al. (2013). Aquaporin-4 expression in post-traumatic syringomyelia. *J Neurotrauma* 30**,** 1457-67. doi: 10.1089/neu.2012.2614.

Hladky, S. B. and Barrand, M. A. (2014). Mechanisms of fluid movement into, through and out of the brain: evaluation of the evidence. *Fluids Barriers CNS* 11**,** 26. doi: 10.1186/2045-8118-11-26.

Iliff, J. J., Goldman, S. A., and Nedergaard, M. (2015). Implications of the discovery of brain lymphatic pathways. *Lancet Neurol* 14**,** 977-9. doi: 10.1016/S1474-4422(15)00221-5.

Iliff, J. J., et al. (2012). A paravascular pathway facilitates CSF flow through the brain parenchyma and the clearance of interstitial solutes, including amyloid beta. *Sci Transl Med* 4**,** 147ra11. doi: 10.1126/scitranslmed.3003748.

Klekamp, J. (2002). The pathophysiology of syringomyelia - historical overview and current concept. *Acta Neurochir (Wien)* 144**,** 649-64. doi: 10.1007/s00701-002-0944-3.

Milhorat, ThomasH, Johnson, RichardW, and Johnson, WalterD (1991), 'Evidence of CSF Flow in Rostral Direction Through Central Canal of Spinal Cord in Rats', in Satoshi Matsumoto and Norihiko Tamaki (eds.), *Hydrocephalus* (Springer Japan), 207-17.

Peschanski, M. and Ralston, H. J., 3rd (1985). Light and electron microscopic evidence of transneuronal labeling with WGA-HRP to trace somatosensory pathways to the thalamus. *J Comp Neurol* 236**,** 29-41. doi: 10.1002/cne.902360104.

Rennels, M. L., Blaumanis, O. R., and Grady, P. A. (1990). Rapid solute transport throughout the brain via paravascular fluid pathways. *Adv Neurol* 52**,** 431-9.

Rennels, M. L., et al. (1985). Evidence for a 'paravascular' fluid circulation in the mammalian central nervous system, provided by the rapid distribution of tracer protein throughout the brain from the subarachnoid space. *Brain Res* 326**,** 47-63.

Sakushima, K., et al. (2013). Different surgical treatment techniques used by neurosurgeons and orthopedists for syringomyelia caused by Chiari I malformation in Japan. *J Neurosurg Spine* 18**,** 588-92. doi: 10.3171/2013.3.SPINE12837.

Sharma, Mudit, Coppa, Nicholas, and Sandhu, Faheem A. (2006). Syringomyelia: A Review. *Seminars in Spine Surgery* 18**,** 180-84. doi: http://dx.doi.org/10.1053/j.semss.2006.06.008.

Simon, M. J. and Iliff, J. J. (2015). Regulation of cerebrospinal fluid (CSF) flow in neurodegenerative, neurovascular and neuroinflammatory disease. *Biochim Biophys Acta*. doi: 10.1016/j.bbadis.2015.10.014.

Stoodley, M. A., Jones, N. R., and Brown, C. J. (1996). Evidence for rapid fluid flow from the subarachnoid space into the spinal cord central canal in the rat. *Brain Res* 707**,** 155-64.

Vitellaro-Zuccarello, L., et al. (2005). Distribution of Aquaporin 4 in rodent spinal cord: relationship with astrocyte markers and chondroitin sulfate proteoglycans. *Glia* 51**,** 148-59. doi: 10.1002/glia.20196.

Wagner, H. J., Barthel, J., and Pilgrim, C. (1983). Permeability of the external glial limiting membrane of rat parietal cortex. *Anat Embryol (Berl)* 166**,** 427-37.

Yang, B., Zhang, H., and Verkman, A. S. (2008). Lack of aquaporin-4 water transport inhibition by antiepileptics and arylsulfonamides. *Bioorg Med Chem* 16**,** 7489-93. doi: 10.1016/j.bmc.2008.06.005.